

Scalar Mesons in Charm Decays

Jonathan L. Rosner

Enrico Fermi Institute, University of Chicago, Chicago, IL 60637

Abstract. Results on light scalar mesons in charmed particle decays studied by the CLEO Collaboration at the Cornell Electron Storage Ring are reviewed.

Keywords: Charmed mesons; scalar mesons; Dalitz plots

PACS: 13.25.Ft, 14.40.Lb, 14.40.Cs, 11.80.Et

1. INTRODUCTION

The CLEO Collaboration, working at the Cornell Electron Storage Ring (CESR), has performed studies of charmed meson and charmonium decays, whose three-body final states will yield rich information on low-mass scalar resonances once fully analyzed. We have observed the $f_0(980)$ and $a_0(980)$, broad S-wave amplitudes “ $\sigma(600)$ ” and “ $\kappa(800)$ ” in $\pi\pi$ and $K\pi$, and evidence for $f_0(1370) \rightarrow \pi\pi$. Data sets include open charm production near 10 GeV, 27.5 million $\psi(2S)$ as a source of χ_c states and about 6 million tagged $\pi^+\pi^-J/\psi$, $818 \pm 8 \text{ pb}^{-1}$ at $\psi(3770)$ leading to more than 5 million very clean $D\bar{D}$ pairs, and about 600 pb^{-1} at 4170 MeV, yielding about 570 thousand $D_s\bar{D}_s$ pairs. Production mechanisms can affect the determination of resonance parameters (especially for broad states). In this report we give some examples of CLEO’s results on scalar mesons obtained from charmed meson and charmonium decays.

2. EXAMPLES OF CHANNELS

CLEO has data on a wide variety of three-body charmed meson and charmonium decays. These include the following:

- $D^+ \rightarrow K^- \pi^+ \pi^+$ [1]: Is there a κ in the low-energy $K\pi$ S wave?
- $D^0 \rightarrow K_S \pi^+ \pi^-$: CLEO’s sample of 9 fb^{-1} near 10 GeV needed no σ , κ [2] but BaBar [3] and Belle [4] have $m(\sigma_1) \simeq 500 \text{ MeV}$, $m(\sigma_2) \simeq 1037 \text{ MeV}$.
- $D^0 \rightarrow \pi^0 \pi^+ \pi^-$ is dominated by ρ^\pm, ρ^0 bands [5].
- $D^+ \rightarrow \pi^- \pi^+ \pi^+$: scalars appear to be important [6].
- $D^0 \rightarrow K^+ K^- \pi^0$: A $K\pi$ S-wave amplitude is needed [7].
- $D^0 \rightarrow K_S \eta \pi^0$: $a_0(980)$, $K^*(892)$ are seen [8].
- $D^+ \rightarrow K^- K^+ \pi^+$: a $K^- \pi^+$ S-wave (e.g., the LASS amplitude [9]) is important.
- $D^0 \rightarrow K_S \pi^0 \pi^0$: Subsystems include $K^*(892)$, $f_0(980)$, $f_0(1370)$, $K^*(1680)$ [10].
- $\chi_{c1} \rightarrow \eta \pi^+ \pi^-$ involves $a_0(980)$, $f_2(1270)$, and $\sigma(500)$; $\chi_{c1} \rightarrow (K^+ K^- \pi^0, \pi^\pm K^\mp K_S)$ involves $K^*(892)$, $K_0^*(1430)$, $K_2^*(1430)$, and $a_0(980)$ [11].

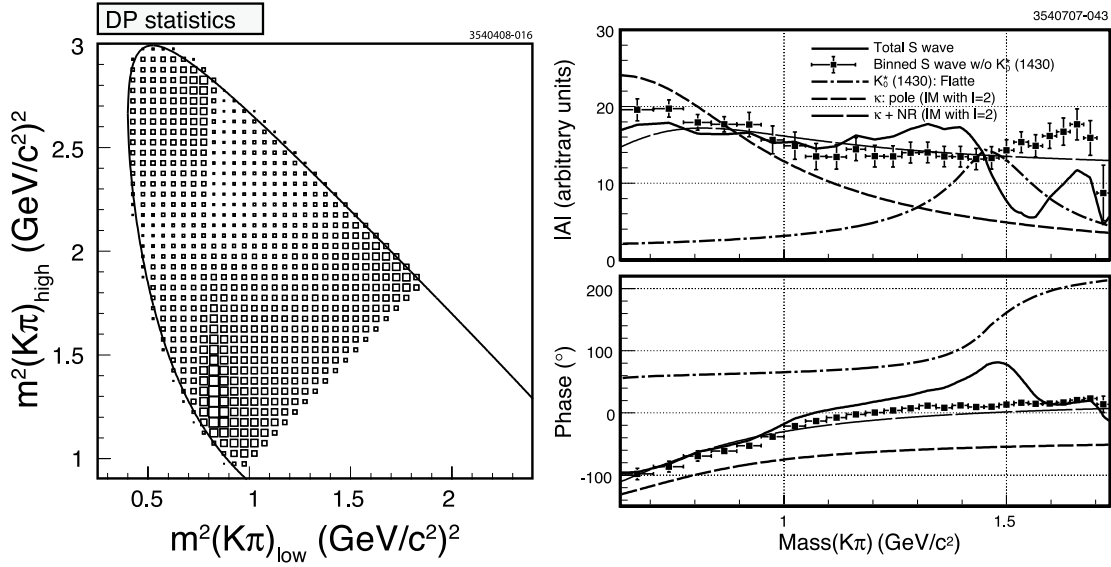


FIGURE 1. Left: Dalitz plot for $D^+ \rightarrow K^- \pi^+ \pi^+$; right: amplitude and phase of $I = 1/2$ $K\pi$ S wave. From Ref. [12].

3. $D^+ \rightarrow K^- \pi^+ \pi^+$

D^+ candidates for $K^- \pi^+ \pi^+$ are selected on the basis of energy and momentum conservation. The sample based on 572 pb^{-1} (about 2/3 of the final total) [12], superseding an earlier one [1] based on 281 pb^{-1} , contains 140793 events with a small background of 1.1%. The largest previous sample was $\sim 15,000$ events from Fermilab E791 [13].

The CLEO Dalitz plot for $D^+ \rightarrow K^- \pi^+ \pi^+$ is shown in Fig. 1. The enhancements on the opposite sides of the $K^*(892)$ band for high and low $m^2(K\pi)_{\text{high}}$ indicate interference with an amplitude of opposite parity to $K^*(892)$ (likely an S wave). Several fits all have a prominent low- $m(K\pi)$ S-wave amplitude. A quasi-model-independent partial wave analysis (QMIPWA; cf. [13]) has a κ -like behavior, but displaced in overall phase.

In fits to the Dalitz plot, a κ pole position depends on whether its Breit-Wigner width Γ is constant or energy-dependent. The QMIPWA determines the S-wave $K\pi$ amplitude and phase for 26 $m^2(K\pi)$ bins; the result resembles the κ + nonresonant amplitude obtained in other fits. A high- $m(\pi\pi)$ contribution from an $I_{\pi\pi} = 2$ amplitude, perhaps due to $\pi^+ \pi^+ \rightarrow \rho^+ \rho^+$, is required for a good fit. In fits with a κ , the S-wave phase does not go through 90° exactly at the resonance mass. When κ is represented by a complex pole (equivalent to a constant Breit-Wigner width), the $\kappa\pi^+$ fit fraction is $\sim 20\%$.

Scalar strange resonances couple much more strongly to $K\eta'$ than to $K\eta$ [14]. In a limit (corresponding to a particular octet-singlet mixing) where $\eta \simeq (u\bar{u} + d\bar{d} - s\bar{s})/\sqrt{3}$; $\eta' \simeq (u\bar{u} + d\bar{d} + 2s\bar{s})/\sqrt{6}$, the contributions of strange and nonstrange quarks in η cancel exactly in $K_0^* \rightarrow K\eta$ while they add constructively in $K_0^* \rightarrow K\eta'$. This is the same physics that favors $B \rightarrow K\eta'$ over $B \rightarrow K\eta$. The pattern would be reversed for vector strange resonances. Thus $K_0^*(1430)$ should be strongly associated with the nearby $K\eta'$ threshold; the $K\pi$ S wave should become inelastic only above this energy. One then might expect a zero (a manifestation of the Ramsauer-Townsend effect!) in the scalar

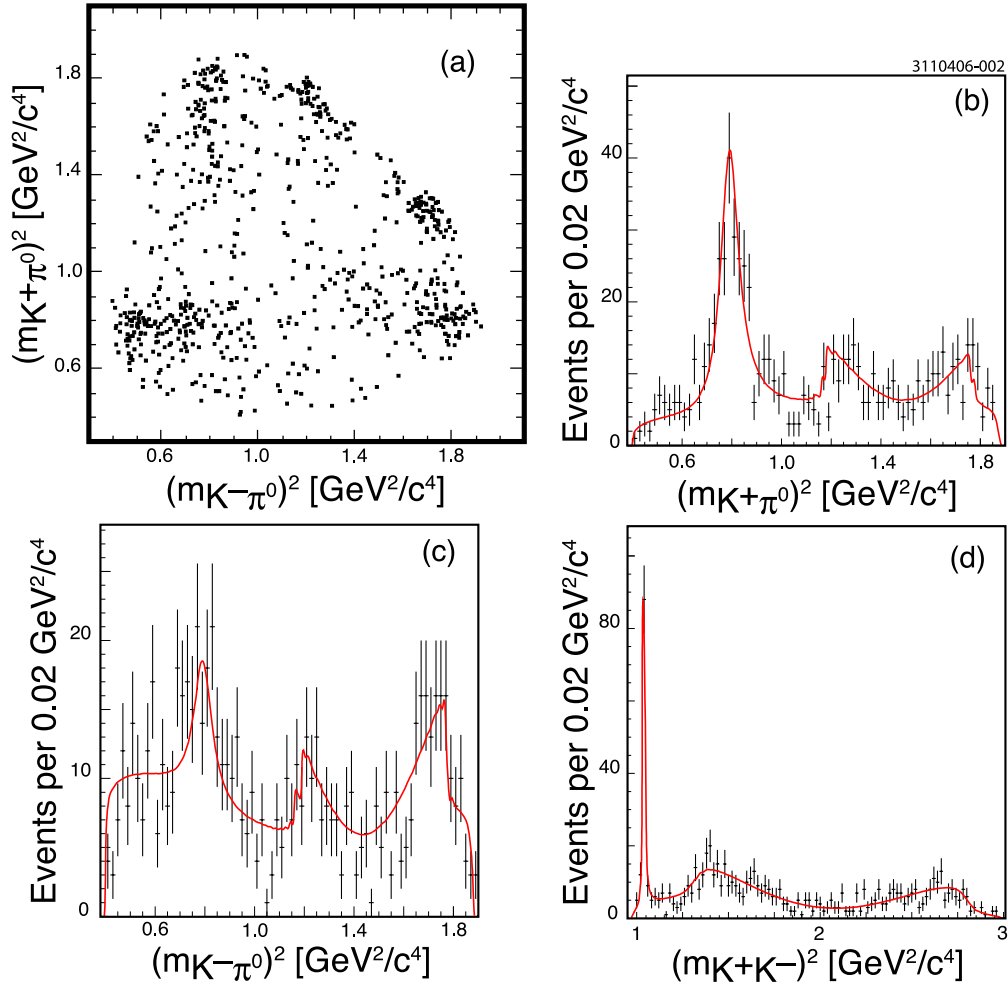


FIGURE 2. (a) Dalitz plot for $D^0 \rightarrow K^+K^-\pi^0$ and projections on (b) $m_{K^+\pi^0}^2$; (c) $m_{K^-\pi^0}^2$; (d) $m_{K^+K^-}^2$. From Ref. [7]. Curves denote a fit with $K^*(892)$, ϕ , and nonresonant S wave.

$I = 1/2$ $K\pi$ amplitude below $K_0^*(1430)$ if a low-mass κ exists.

CLEO and E791 find the $K_0^*(1430)$ heavier ($m \simeq 1460$ MeV) and narrower ($\Gamma \simeq 175$ MeV) than the PDG world average from 2006 [15] (1414 ± 6 MeV, 290 ± 21 MeV, based mainly on elastic $K\pi$ scattering [9]). BES [16] find a scalar $K\pi$ resonance in $\chi_{c0} \rightarrow \pi^+\pi^-K^+K^-$ with $m = (1455 \pm 20 \pm 15)$ MeV, $\Gamma = 270 \pm 45_{-30}^{+35}$ MeV.

4. $D^0 \rightarrow K^+K^-\pi^0$

A sample of 735 $D^0 \rightarrow K^+K^-\pi^0$ candidates was obtained with the CLEO III detector using 9.0 fb^{-1} at 10.58 GeV. The corresponding Dalitz plot and its projections are shown in Fig. 2. One sees opposite signs of the interference between K^\pm and a large S-wave amplitude (typical fit fraction 20–40%), implying opposite relative phases for $D^0 \rightarrow (K^{*+}K^-, K^{*-}K^+)$. Although the $K\pi$ S wave is appreciable, one cannot tell if it

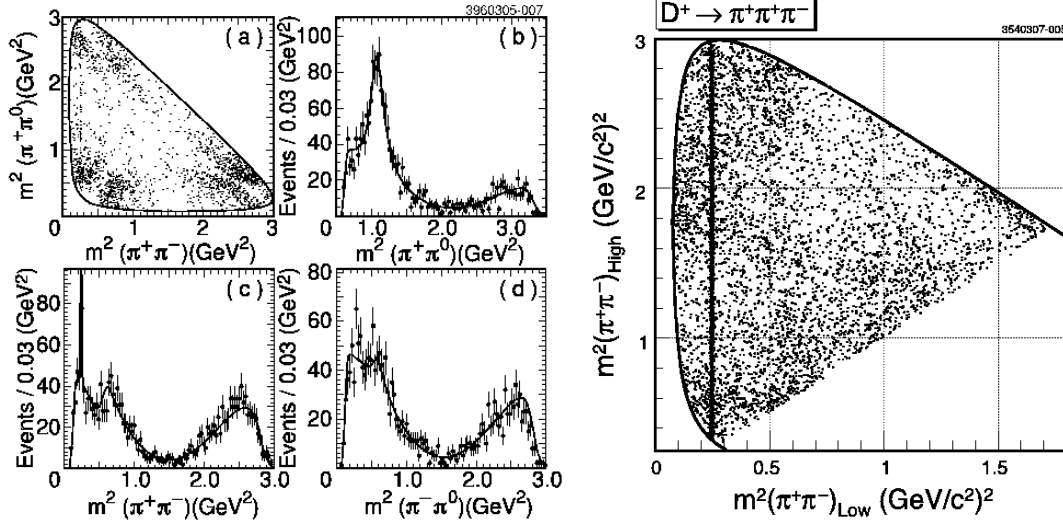


FIGURE 3. Left: (a) Dalitz plot for $D^0 \rightarrow \pi^+ \pi^- \pi^0$; (b) $m^2_{\pi^+ \pi^0}$ projection; (c) $m^2_{\pi^+ \pi^-}$ projection; (d) $m^2_{\pi^- \pi^0}$ projection. Right: Dalitz plot for $D^+ \rightarrow \pi^+ \pi^+ \pi^-$. The dark vertical band is due to $K_S \rightarrow \pi^+ \pi^-$.

is resonant. A curious dip in $m(K\pi)$ occurs around 1 GeV. Could this be a Ramsauer-Townsend zero between a κ and $K_0^*(1430)$? The BaBar Collaboration [17] has $> 11,000$ events in a 385 fb^{-1} sample, with no dip seen.

5. $D^0 \rightarrow \pi^+ \pi^- \pi^0$ VS. $D^+ \rightarrow \pi^- \pi^+ \pi^+$

CLEO $D^0 \rightarrow \pi^+ \pi^- \pi^0$ data are based on 9 fb^{-1} near 10 GeV [5], while $D^+ \rightarrow \pi^- \pi^+ \pi^+$ data are based on 281 pb^{-1} sample (about 1/3 of the final total) at the $\psi(3770)$ [6]. Their Dalitz plots are compared in Fig. 3. While $D^0 \rightarrow \pi^+ \pi^- \pi^0$ is dominated by ρ^\pm, ρ^0 , $D^+ \rightarrow \pi^- \pi^+ \pi^+$ can have only ρ^0 , not produced by the charged weak current, so it is not surprising that the scalar fit fraction is larger in this decay. For D^0 it is found to be $< 4\%$; for D^+ it is 40–80%.

6. $D^0 \rightarrow K_S \pi^0 \pi^0$

A preliminary analysis of $D^0 \rightarrow K_S \pi^0 \pi^0$ based on 281 pb^{-1} taken by CLEO at $\psi(3770)$ [10] obtains fit fractions in the Dalitz plot [Fig. 4, showing $m^2(\pi^0 \pi^0)$ vs. $m^2(K_S \pi^0)$] of $(54.2 \pm 5.4 \pm 3.0 \pm 5.0)\%$ for $K^*(892)$, $(9.0 \pm 3.2 \pm 0.9 \pm 2.7)\%$ for $f_0(980)$, $(23.8 \pm 7.1 \pm 4.7 \pm 8.6)\%$ for $f_0(1370)$, and $(11.4 \pm 2.7 \pm 2.1 \pm 3.2)\%$ for a $K^*(1680)$ with spin 1. Judgment on a low-mass σ awaits analysis of the full 818 pb^{-1} data sample.

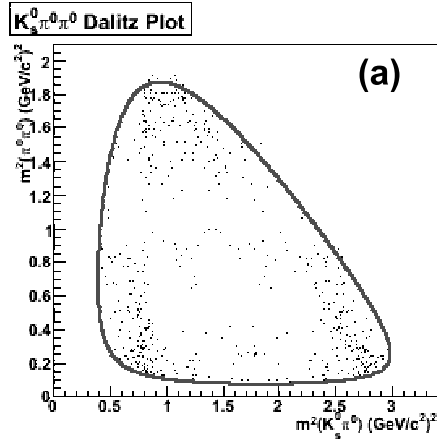


FIGURE 4. Dalitz plot for $D^0 \rightarrow K_S \pi^0 \pi^0$.

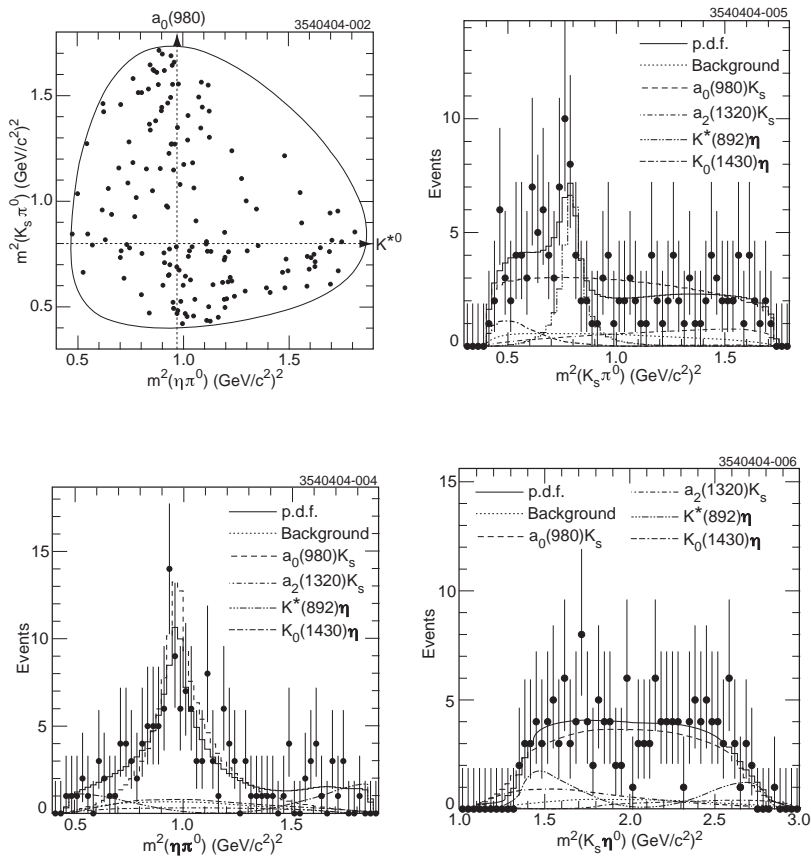


FIGURE 5. Upper left: Dalitz plot for $D^0 \rightarrow K_S \eta \pi^0$; upper right: $m_{K_S \pi^0}^2$ projection; lower left: $m_{\eta \pi^0}^2$ projection; lower right: $m_{K_S \eta}^2$ projection.

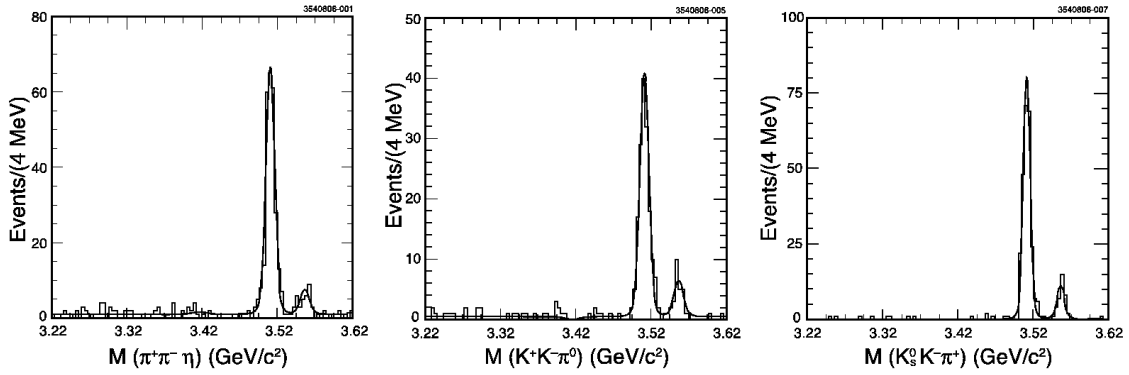


FIGURE 6. Mass distributions for final states X in $\psi(2S) \rightarrow \gamma X$. Left: $X = \pi^+\pi^-\eta$; middle: $X = K^+K^-\pi^0$; right: $X = K_S^0K^-\pi^+$.

7. $D^0 \rightarrow K_S\eta\pi^0$

Published CLEO data on $D^0 \rightarrow K_S\eta\pi^0$ come from 9.0 fb^{-1} near the $\Upsilon(4S)$, yielding a signal of 155 ± 22 events. The Dalitz plot (Fig. 5) is dominated by $a_0(980)K_S$ [fit fraction $\mathcal{O}(1)$]. The $K^*(892)\eta$ fit fraction is $\simeq 30\%$. It would be interesting to compare $D^0 \rightarrow K_S a_0^0$ with $D^0 \rightarrow K^- a_0^+$ and $D^+ \rightarrow K_S a_0^+$. Related processes are $D^0 \rightarrow \bar{\kappa}^0\pi^0$, $D^0 \rightarrow \kappa^-\pi^+$, and $D^+ \rightarrow \bar{\kappa}^0\pi^+$ if κ and a_0 belong to the same SU(3) multiplet. The $\psi(3770)$ data set will contain $\sim 1200 K_S\pi^0\eta$, $\sim 8000 K^-\pi^+\eta$, and $\sim 5000 K_S\pi^+\eta$.

8. THREE-BODY χ_c DECAYS

The transitions $\psi(2S) \rightarrow \gamma\chi_{cJ}$ ($J = 0, 1, 2$) were studied by CLEO, reconstructing exclusive final states for 3 million $\psi(2S)$ [11] (24.5 million more $\psi(2S)$ are under analysis). The signals are shown in Fig. 6. The three-body decays $\chi_{c1} \rightarrow (\eta\pi^+\pi^-, K^+K^-\pi^0, K_S K^\pm\pi^\mp)$ have enough events (255_{-16}^{+17} , 157 ± 13 , and 249 ± 16 , respectively) for Dalitz plot analyses. In these channels $I_{\pi\pi} = 0$ in $\chi_{c1} \rightarrow \eta\pi^+\pi^-$ and $I_{K\bar{K}} = 1$ in $\chi_{c1} \rightarrow (K^+K^-\pi^0, K_S K^\pm\pi^\mp)$. The analysis of the 3 million $\psi(2S)$ did not consider χ_{c1} polarization or interference between resonances, desirable features in analysis of the full sample.

8.1. $\chi_{c1} \rightarrow \eta\pi^+\pi^-$

The Dalitz plot for $\chi_{c1} \rightarrow \eta\pi^+\pi^-$ and its projections are shown in Fig. 7. The fit fractions, in percent, are $75.1 \pm 3.5 \pm 4.3$ for $a_0(980)^\pm\pi^\mp$, $14.4 \pm 3.1 \pm 1.9$ for $f_2(1270)\eta$, and $10.5 \pm 2.4 \pm 1.2$ for $\sigma\eta$. Here σ is parametrized by a complex pole at $(511 \pm 28 - i102 \pm 50) \text{ MeV}$. The low-mass $\pi\pi$ enhancement is visible both in the Dalitz plot and in the $m^2(\pi^+\pi^-)$ projection. Flavor SU(3) would imply that $\chi_{c1} \rightarrow \kappa\bar{K}$ should be visible if $\chi_{c1} \rightarrow a_0\pi$ is so prominent.

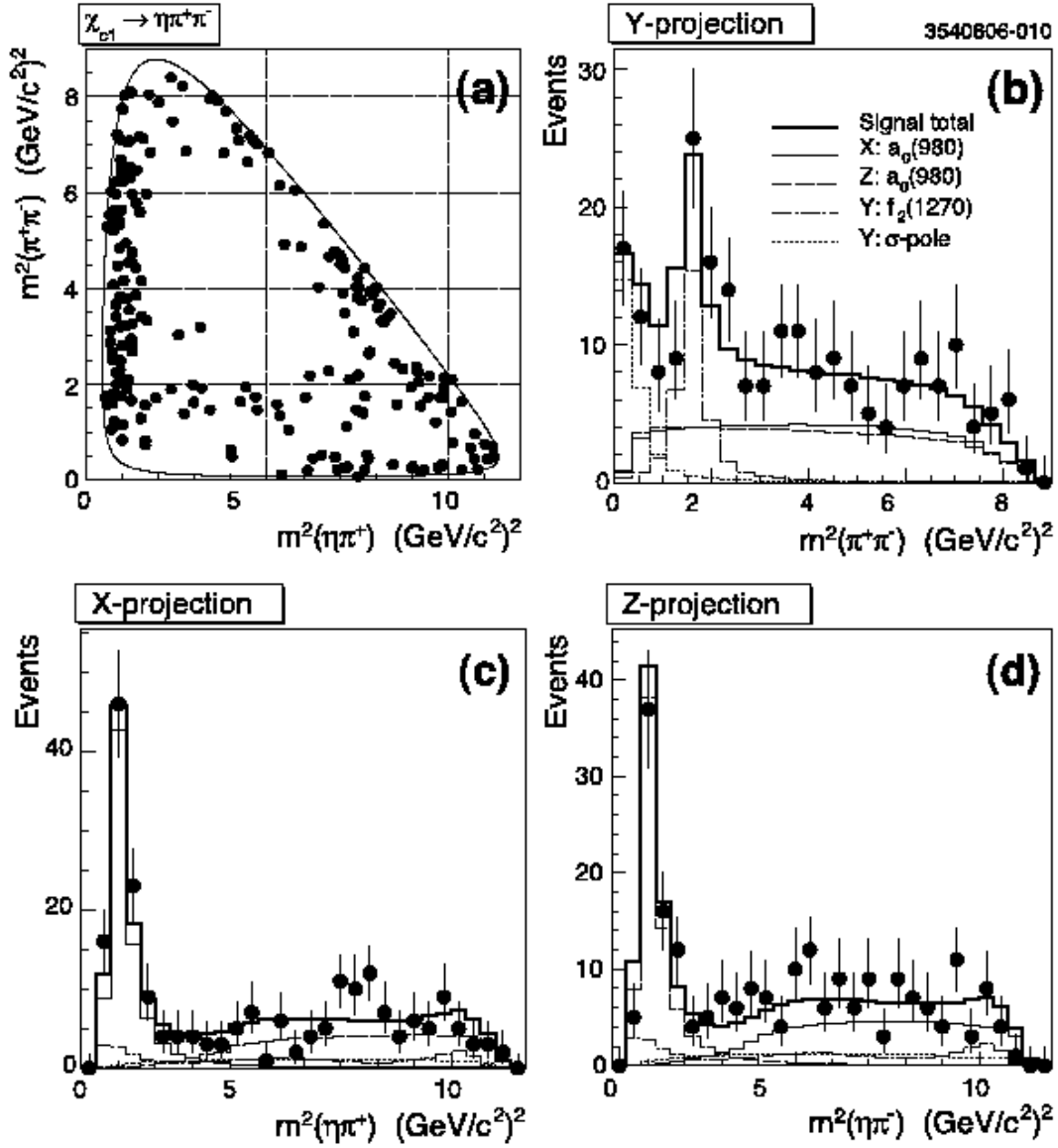


FIGURE 7. (a) Dalitz plot for $\chi_{c1} \rightarrow \eta \pi^+ \pi^-$ and projections on (b) $m_{\pi^+ \pi^-}^2$; (c) $m_{\eta \pi^+}^2$; (d) $m_{\eta \pi^-}^2$. Main contributions to $m_{\pi^+ \pi^-}^2$ projection are σ and $f_2(1270)$; main contributions to $m_{\eta \pi^\pm}^2$ projections are $a_0(980)^\pm$.

8.2. $\chi_{c1} \rightarrow (K^+ K^- \pi^0, K_S K^\pm \pi^\mp)$

The Dalitz plots for $\chi_{c1} \rightarrow (K^+ K^- \pi^0, K_S K^\pm \pi^\mp)$ and their projections are shown in Figs. 8 and 9. In analyzing them the $I = 0$ channels of $K^+ K^- \pi^0$ and $K_S K^\pm \pi^\mp$, related by isospin, have been combined. The fit fractions, in percent, are $31.2 \pm 2.2 \pm 1.7$ for $K^*(892) \bar{K}$, $30.4 \pm 3.5 \pm 3.7$ for $K_0^*(1430) \bar{K}$, $23.1 \pm 3.4 \pm 7.1$ for $K_2^*(1430) \bar{K}$, and $15.1 \pm 2.7 \pm 1.5$ for $a_0(980) \pi$. The addition of a κ or nonresonant $K \pi$ S-wave doesn't

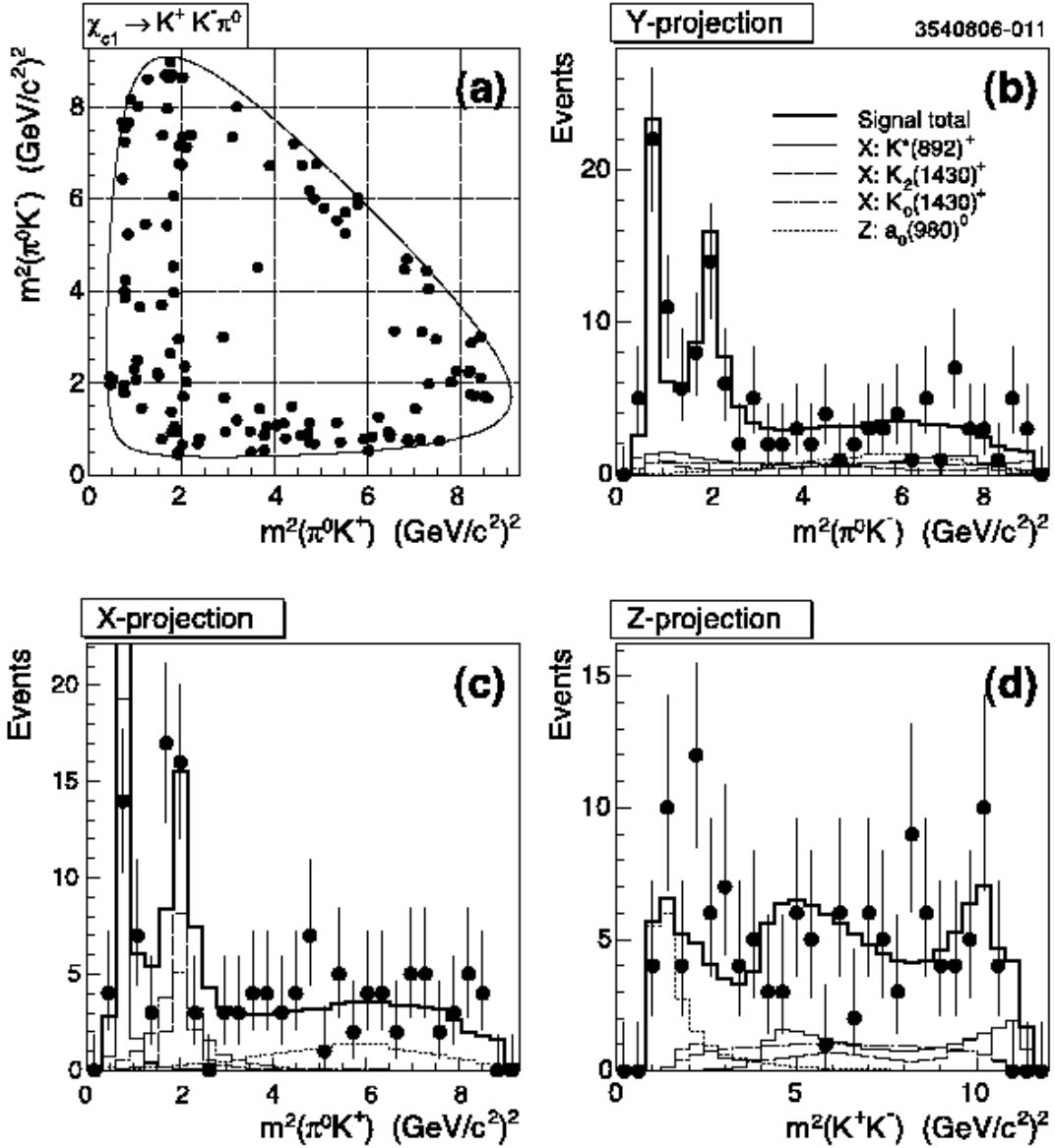


FIGURE 8. (a) Dalitz plot for $\chi_{c1} \rightarrow K^+ K^- \pi^0$ and projections on (b) $m_{\pi^0 K^-}^2$; (c) $m_{\pi^0 K^+}^2$; (d) $m_{K^+ K^-}^2$. Main contributions to $m_{\pi^0 K^\pm}^2$ projections are $K^*(892)^+$, $K_2(1430)^+$, and $K_0(1430)^+$; main contribution to $m_{K^+ K^-}^2$ projection is $a_0(980)^0$.

improve the fit quality. However, account of interference might show a low-mass $K\pi$ S wave as in the analysis of $D^+ \rightarrow K^- \pi^+ e^+ \nu_e$ [18].

For $\chi_{c1} \rightarrow K_S K^\pm \pi^\mp$ one expects twice as many events as in $\chi_{c1} \rightarrow K^+ K^- \pi^0$, neglecting efficiency differences. In the full data set the expected sample of ~ 2000 $\chi_{c1} \rightarrow \eta \pi^+ \pi^-$ should permit a good determination of the “ σ ” properties. We expect many other three-body χ_{cJ} final states to be reconstructed in the full CLEO $\psi(2S)$ radiative decay sample.

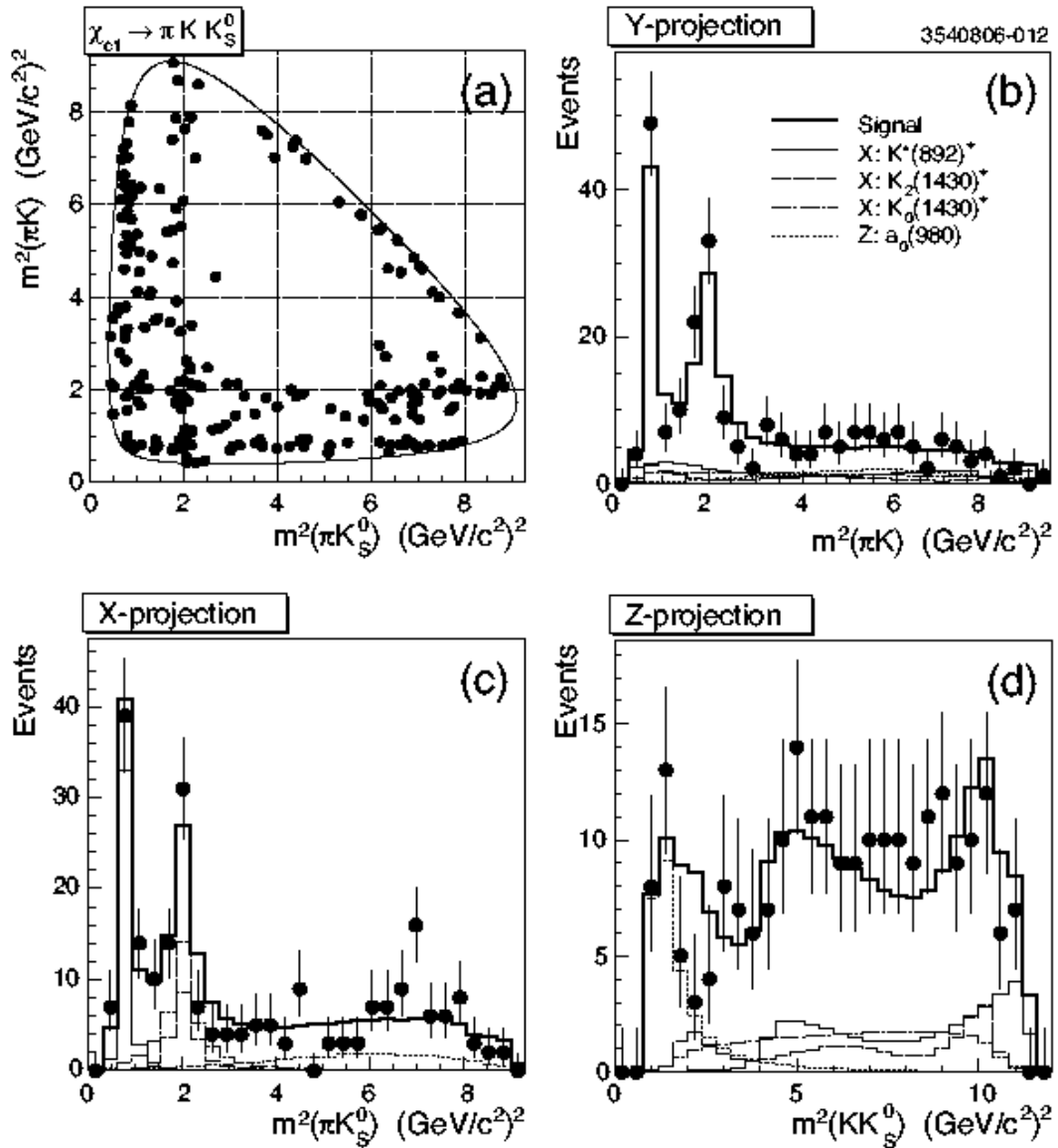


FIGURE 9. (a) Dalitz plot for $\chi_{c1} \rightarrow K_S K^\pm \pi^\mp$ and projections on (b) $m_{\pi^\pm K^\mp}^2$; (c) $m_{\pi^\pm K_S}^2$; (d) $m_{K^\pm K_S}^2$. Main contributions are as in Fig. 8.

9. CONCLUSIONS

Charmed meson and charmonium decays can be a rich source of information on scalar resonances between pairs of pseudoscalar mesons. The data from CLEO show the potential of these channels. The $a_0(980)$ and $f_0(980)$ are without question in CLEO data; $\kappa(800)$ and $\sigma(600)$ make sporadic appearances. Their inferred masses and widths depend on production channels and line shape models. Because of Bose statistics, the σ ($I_{\pi\pi} = 0$) is easier to isolate than the κ ($I_{K\pi} = 1/2$). Although not related to charm

decays, it is notable that CLEO needs a σ in describing $\tau \rightarrow \pi\pi^0\pi^0\nu$ [19]. Tests of whether the $a_0(980)$ and $f_0(980)$ belong to a nonet with $\kappa(800)$ and $\sigma(600)$ are available in charmonium (e.g., χ_{c1}) decays. We look forward to the realization of CLEO's ultimate potential for shedding light on scalar mesons with the analysis of the full data sets from $\psi(2S)$, $\psi(3770)$, and $E_{\text{cm}} = 4170$ MeV.

ACKNOWLEDGMENTS

I thank my colleagues on CLEO and particularly Mikhail Dubrovin for much valuable advice, and the organizers of this Workshop for providing a stimulating environment for discussion. This work was supported in part by the United States Department of Energy under Grant No. DE FG02 90ER40560.

REFERENCES

1. G. Bonvicini *et al.* [CLEO Collaboration], CLEO-CONF 07-01, arXiv:0707.3060 [hep-ex].
2. H. Muramatsu *et al.* [CLEO Collaboration], *Phys. Rev. Lett.* **89**, 251802 (2002) [Erratum-*ibid.* **90**, 059901 (2003)].
3. M. Pappagallo [BaBar Collaboration], SLAC-PUB-12983, published in *Acta Phys. Polon. B* **38**, 2885 (2007).
4. A. Poluektov *et al.* [Belle Collaboration], *Phys. Rev. D* **73**, 112009 (2006).
5. D. Cronin-Hennessy *et al.* [CLEO Collaboration], *Phys. Rev. D* **72**, 031102 (2005) [Erratum-*ibid.* **D75**, 119904 (2007)].
6. G. Bonvicini *et al.* [CLEO Collaboration], *Phys. Rev. D* **76**, 012001 (2007).
7. C. Cawfield *et al.* [CLEO Collaboration], *Phys. Rev. D* **74**, 031108 (2006).
8. P. Rubin *et al.* [CLEO Collaboration], *Phys. Rev. Lett.* **93**, 111801 (2004).
9. D. Aston *et al.* [LASS Collaboration], *Nucl. Phys.* **B296**, 496 (1988).
10. P. Naik, L. Zhang and N. Lowrey [CLEO Collaboration], presented at HADRON 07, arXiv:0712.2266.
11. S. B. Athar *et al.* [CLEO Collaboration], *Phys. Rev. D* **75**, 032002 (2007).
12. G. Bonvicini *et al.* [CLEO Collaboration], arXiv:0802.4214 [hep-ex].
13. E. M. Aitala *et al.* [Fermilab E791 Collaboration], *Phys. Rev. Lett.* **89**, 121801 (2002); *Phys. Rev. D* **73**, 032004 (2006); *ibid.* **74**, 059901(E) (2006).
14. H. J. Lipkin, *Phys. Rev. Lett.* **46**, 1307 (1981); *Phys. Lett. B* **254**, 247 (1991).
15. W.-M. Yao *et al.* [Particle Data Group], *J. Phys. G* **33**, 1 (2006).
16. M. Ablikim *et al.* [BES Collaboration], *Phys. Rev. D* **72**, 092002 (2005).
17. B. Aubert *et al.* [BABAR Collaboration], *Phys. Rev. D* **76**, 011102 (2007).
18. M. R. Shepherd *et al.* [CLEO Collaboration], *Phys. Rev. D* **74**, 052001 (2006).
19. D. M. Asner *et al.* [CLEO Collaboration], *Phys. Rev. D* **61**, 012002 (2000).